JACS
JOURNAL OF THE AMERICAN CHEMICAL SOCIETY
Article
pubs.acs.org/JACS

Transition State Analysis of *Vibrio cholerae* Sialidase-Catalyzed Hydrolyses of Natural Substrate Analogues

Jefferson Chan,[†] Andrew R. Lewis,[†] Deepani Indurugalla,[†] Melissa Schur,[‡] Warren Wakarchuk,[‡] and Andrew J. Bennet*,[†]

[†]Department of Chemistry, Simon Fraser University, 8888 University Drive, Burnaby, British Columbia, V5A 1S6, Canada
[‡]Institute for Biological Sciences, National Research Council Canada, Ottawa, Ontario, Canada

Supporting Information

ABSTRACT: A series of isotopically labeled natural substrate analogues (phenyl 5-*N*-acetyl-α-D-neuraminyl-(2→3)-β-D-galactopyranosyl-(1→4)-1-thio-β-D-glucopyranoside; Neu5Acα2,3Lacβ SPh, and the corresponding 2→6 isomer) were prepared chemoenzymatically in order to characterize, by use of multiple kinetic isotope effect (KIE) measurements, the glycosylation transition states for *Vibrio cholerae* sialidase-catalyzed hydrolysis reactions. The derived KIEs for Neu5Acα2,3Lacβ SPh for the ring oxygen ($^{18}V/K$), leaving group oxygen ($^{18}V/K$), C3-*S* deuterium ($^{D}V/K_S$) and C3-*R* deuterium ($^{D}V/K_R$) are 1.029 ± 0.002, 0.983 ± 0.001, 1.034 ± 0.002, and 1.043 ± 0.002, respectively. In addition, the KIEs for Neu5Acα2,6β SPh for C3-*S* deuterium ($^{D}V/K_S$) and C3-*R* deuterium ($^{D}V/K_R$) are 1.021 ± 0.001 and 1.049 ± 0.001, respectively. The glycosylation transition state structures for both Neu5Acα2,3Lacβ SPh and Neu5Acα2,6Lacβ SPh were modeled computationally using the experimental KIE values as goodness of fit criteria. Both transition states are late with largely cleaved glycosidic bonds coupled to pyranosyl ring flattening ($^{4}H_5$ half-chair conformation) with little or no nucleophilic involvement of the enzymatic tyrosine residue. Notably, the transition state for the catalyzed hydrolysis of Neu5Acα2,6β SPh appears to incorporate a lesser degree of general-acid catalysis, relative to the 2,3-isomer.

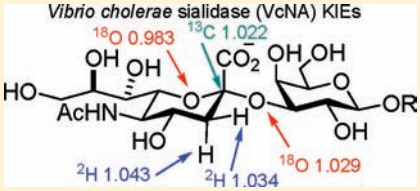

INTRODUCTION

Vibrio cholerae, a Gram-negative bacterium, is responsible for cholera, an illness characterized by acute diarrhea that can result in death due to severe dehydration.[1] Although cholera is a readily treatable disease, involving rehydration therapy, it continues to be a serious health concern in many third-world nations when its presence and impact are especially evident after a natural disaster (i.e., 2010 Haitian earthquake).[2,3] The outbreak in Haiti is part of the ongoing seventh cholera pandemic.[4] Such pandemics are typically associated with a breakdown of the water and sanitation infrastructure. Upon infection, *V. cholerae* aggressively secretes an enterotoxin which binds to the GM_1 ganglioside of enterocyte microvilli.[5] The cholera toxin (CT) gains entry into the cell through this interaction and triggers a cyclic adenosine monophosphate (cAMP) mediated disruption of the enterocyte membrane's sodium and chloride ion channels, resulting in hypersecretion of fluids and electrolytes into the intestinal lumen, which causes profuse diarrhea.[5] The bacteria also produces a sialidase (*N*-acetylneuraminosyl glycohydrolase, neuraminidase, EC 3.2.1.18)[6] that processes higher order gangliosides to yield GM_1.[7] A subtle synergistic effect has been reported between the activity of the *V. cholerae* neuraminidase (VcNA) and the binding and uptake of CT.[8] X-ray crystallographic studies reveal that VcNA folds into a central catalytic domain flanked by two carbohydrate-binding modules (CBM),[6] one of which displays a high affinity for α-sialic acid motifs.[9] This CBM is thought to be involved in directing *V. cholerae* to the small intestine where epithelial cells are rich in sialic acid.[10] On the basis of its role in pathogenesis, VcNA is a potential target for drug development.

One approach to drug discovery involves obtaining a detailed understanding of the mechanism of action of the target enzyme and this can be achieved by measuring a comprehensive set of kinetic isotope effects (KIEs) followed by solving the TS structure using ab initio methods.[11,12] Such studies can be used to analyze various key transition state (TS) features, including: pyranosyl ring geometry, charge development and the degree of bond cleavage and/or formation. These TS characteristics can then be used as a blueprint for the design of tight-binding TS analogue inhibitors by matching the calculated Molecular Electrostatic Potential (MESP) map of the TS to those of the candidate inhibitors.[13] With regard to VcNA, KIE measurements have been reported by Guo and Sinnott using an activated substrate, *p*-nitrophenyl α-sialoside **1**.[14] These authors measured leaving group ^{18}O-KIEs on the kinetic parameters V/K and V, as well as β-secondary deuterium KIEs.[14] However, it is well-known that activated substrates alter the free energy profile of an enzyme-catalyzed reaction, and thus, they can lessen, or even obviate, the need for a type of catalysis,[15] such as general acid catalysis as is the case for the good leaving group *p*-nitrophenoxide. As a result, mechanistic deductions made with activated substrates can, in certain cases, be misleading.

Recently, the determination of an anomeric ^{13}C-KIE for the VcNA-catalyzed hydrolysis of the natural substrate analogue

Received: September 10, 2011
Published: February 1, 2012

   dx.doi.org/10.1021/ja208564y | *J. Am. Chem. Soc.* 2012, 134, 3748–3757

Neu5Acα2,3LacβSPh (**2**) and the anomeric ^{13}C-, a ring-oxygen ^{18}O-, and a leaving group ^{18}O-KIEs were reported for the hydrolysis of the isomeric Neu5Acα2,6LacβSPh (**3**).[16] The current study details additional heavy-atom KIE measurements on the isomeric 2,3-linked natural substrate analogue Neu5Acα2,3LacβSPh and the associated β-secondary deuterium KIEs for both 2,3- and 2,6-substrates. In addition, quantum chemical calculations were used to model the glycosylation TS structures for the VcNA-catalyzed hydrolysis of **2** and **3**.

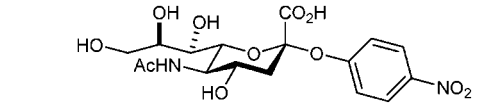

1

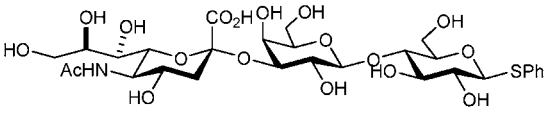

2

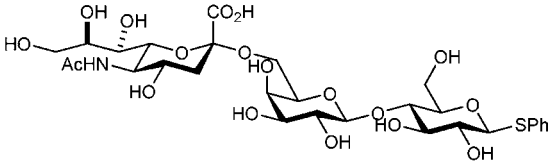

3

EXPERIMENTAL METHODS

General. Cytidine 5′-triphosphate disodium salt was purchased from 3B Scientific Corporation. Thiophenol (≥99%) was purchased from Aldrich. *N*,*N*-Dimethylformamide (anhydrous, amine free, 99.9%) was purchased from Alfa Aesar. ^{13}C-labeled sodium pyruvates (>99.0 atom % C-13) were purchased from Cambridge Isotopes and ^{18}O-labeled H_2O was purchased from Marshall Isotopes (95.1 atom % O-18, batch no. 020414nw). All other reagents were purchased from Aldrich and used without purification. Thin-layer chromatography (TLC) was performed on aluminum-backed TLC plates precoated with Merck silica gel 60 F254. Compounds were visualized with UV light and/or staining with a *p*-anisaldehyde solution. Flash chromatography was performed using silica gel 60 (230−400 mesh). Solvents used for anhydrous reactions were dried and distilled immediately prior to use. THF was dried and distilled over sodium metal, and dichloromethane was dried and distilled over calcium hydride. For anhydrous reactions, all glassware was flame-dried and cooled under a nitrogen atmosphere immediately prior to use. NMR spectra were recorded on a Bruker AVANCE II 600 MHz spectrometer equipped with a 5 mm QNP cryoprobe. Chemical shifts (δ) are listed in parts per million (ppm) downfield from TMS. The signal residues from deuterated chloroform and external TMS salts (D_2O) were used for ^{1}H NMR spectral references; for ^{13}C NMR spectra, natural abundance signals from $CDCl_3$ and external TMS salts (D_2O) were used as references. All NMR peak assignments are based on ^{1}H−^{1}H COSY and ^{1}H−^{13}C HMQC experiments; coupling constants are reported in hertz (Hz). *Escherichia coli* sialic acid (Neu5Ac) aldolase was purchased from Codexis. *Neisseria meningitidis* CMP-Neu5Ac synthase was expressed and purified as reported.[17] A construct (PDS-06) expressing the α-2,6-sialyltransferase from *Photobacterium* sp. JT-ISH-224[18] was made using a synthetic gene: it was expressed as a fusion protein with the *E. coli* maltose-binding protein (without the leader peptide), and purified on amylose resin according to the manufacturer's instructions (New England Biolabs, Beverly, MA). The *Campylobacter jejuni* Cst-I α-2,3-sialyltransferase was expressed as a full-length protein with an N-terminal maltose binding protein fusion partner (construct CST-06). The enzyme was prepared and purified as previously described.[19] Reaction progress had to be closely monitored to avoid product hydrolysis which occurs at higher product concentrations. Reactions were stopped when reactions reached approximately 90% completion. ($^{18}O_2$)-Benzoic acid[16] and 2-acetamido-2-deoxy-D-(3-^{18}O)mannose[20] were synthesized as reported in the literature. Deuterium exchange into (3-^{13}C) Neu5Ac, which was made from (3-^{13}C)pyruvate using sialic acid aldolase,[21] followed an established protocol.[22] Phenyl 1-thio-β-D-lactoside (**4a**) was prepared in 3 steps from D-lactose in an overall yield of 50%.[23] The general chemoenzymatic synthesis and purification of Neu5Acα2,3LacβSPh **2** and Neu5Acα2,6LacβSPh **3** were previously described.[16] Phenyl (3′-^{18}O)-1-thiolactoside (**4b**) was prepared from the unlabeled thiolactoside; full experimental details are given below.

*Phenyl (3,4-O-Isopropylidene-β-D-galactopyranosyl)-(1→4)-1-thio-β-D-glucopyranoside (**5**).* A solution of **4a** (3.50 g, 8.06 mmol), 2,2-dimethoxypropane (1.7 mL, 13.9 mmol), anhydrous DMF (31 mL), and acetone (65 mL) was treated with conc. H_2SO_4 (90 μL, 1.7 mmol). The reaction mixture was stirred at 60 °C until TLC analysis showed the reaction to be complete, R_f = 0.33 (1:9 v/v MeOH/CH_2Cl_2). Upon removal of the volatiles under reduced pressure, the crude residue was washed with Et_2O (2 × 50 mL) and purified via flash chromatography (1:9 v/v MeOH/CH_2Cl_2) to afford the desired product as a white solid (1.33 g, 4.43 mmol, 55% yield). Mp = 192−193 °C; ^{1}H NMR (600 MHz, MeOD) δ 7.64−7.53 (m, 2H), 7.37−7.24 (m, 3H), 4.63 (d, J = 9.8, 1H), 4.39 (d, J = 8.3, 1H), 4.22 (m, 1H), 4..07 (m, 1H), 3.95 (s, 1H), 3.90 (m, 1H), 3.87−3.74 (m, 3H), 3.58 (dt, J = 8.8, 2.0, 2H), 3.47 (t, J = 7.7, 2H), 3.29 (m, 1H), 1.49 (s, 3H, CH_3), 1.34 (s, 3H, CH_3); ^{13}C NMR (151 MHz, MeOD) δ 133.55, 131.61, 128.47, 127.05, 109.70, 102.66, 87.74, 79.46, 79.06, 79.01, 76.49, 73.97, 73.67, 73.06, 72.15, 61.03, 60.53, 26.99, 25.08.

*Phenyl (2,6-Di-O-acetyl-3,4-O-isopropylidene-β-D-galactopyranosyl)-(1→4)-2,3,6-tri-O-acetyl-1-thio-β-D-glucopyranoside (**6**).* A solution of **5** (810 mg, 1.71 mmol) in pyridine (20.0 mL) was cooled in an ice-bath and treated with acetic anhydride (1.6 mL, 17.1 mmol). The reaction mixture was stirred at room temperature overnight, diluted with dichloromethane (50 mL), and poured into cold water (100 mL). After separation, the organic layer was washed successively with 10% H_2SO_4 (2 × 50 mL), sat. $NaHCO_3$ (2 × 50 mL), and brine (50 mL). Upon drying (Na_2SO_4) and concentration, the crude residue was purified via flash chromatography (1:1 v/v EtOAc/Hexanes) to afford the desired product as a white solid (1.09 g, 1.59 mmol, 93% yield). Mp = 69−70 °C; ^{1}H NMR (600 MHz, $CDCl_3$) δ 7.54−7.42 (m, 2H), 7.36−7.29 (m, 3H), 5.21 (t, J = 9.1, 1H), 4.93 (t, J = 9.7, 1H), 4.85 (m, 1H), 4.68 (d, J = 10.1, 1H), 4.49 (d, J = 10.5, 1H), 4.30 (m, 3H), 4.21−4.09 (m, 3H), 3.93 (s, 1H), 3.72 (t, J = 9.5, 1H), 3.67 (m, 1H), 2.09−2.07 (15H, 5 × CH_3), 1.53 (s, 3H), 1.32 (s, 3H); ^{13}C NMR (151 MHz, $CDCl_3$) δ 170.73, 170.38, 169.91, 169.57, 169.17, 132.78, 132.10, 128.88, 128.20, 110.86, 100.35, 85.66, 76.84, 75.95, 73.44, 73.05, 72.68, 70.89, 70.31, 63.13, 62.40, 27.33, 26.12, 20.84, 20.83, 20.79, 20.71. ESI-MS: 702.24 [$(M + NH_4)^+$].

*Phenyl (2,6-Di-O-acetyl-β-D-galactopyranosyl)-(1→4)-2,3,6-tri-O-acetyl-1-thio-β-D-glucopyranoside (**7**).* A solution of **6** (825 mg, 1.2 mmol) in H_2O (5 mL) and glacial acetic acid (15 mL) was stirred at 70 °C and the reaction progress was monitored by TLC analysis, R_f = 0.43 (1:9 v/v MeOH/CH_2Cl_2). Upon completion of the reaction, sufficient sat. $NaHCO_3$ was added in order to neutralize the reaction mixture. After extraction with CH_2Cl_2 (3 × 50 mL), the combined organic layers were dried (Na_2SO_4) and concentrated under reduced pressure. The crude residue was purified via flash chromatography (1:19 v/v MeOH/CH_2Cl_2) to afford the desired product as a colorless syrup (660.1 mg, 1.0 mmol, 85% yield). ^{1}H NMR (600 MHz, $CDCl_3$) δ 7.52−7.46 (m, 2H), 7.34−7.28 (m, 3H), 5.19 (t, J = 9.1, 1H), 4.93 (m, 1H), 4.81 (dd, J = 7.9, 9.6, 1H), 4.68 (d, J = 10.1, 1H), 4.54 (dd, J = 1.9, 11.8, 1H), 4.35 (m, 2H), 4.23 (dd, J = 6.4, 11.4, 1H), 4.17 (dd, J = 5.9, 11.8, 1H), 3.83 (d, J = 3.0, 1H), 3.73 (m, 1H), 3.66 (m, 1H), 3.64−3.57 (m, 2H), 2.12 (s, 3H), 2.10 (s, 3H), 2.09 (s, 3H), 2.08 (s, 3H), 2.03 (s, 3H); ^{13}C NMR (151 MHz, $CDCl_3$) δ 171.79, 171.06,

dx.doi.org/10.1021/ja208564y | J. Am. Chem. Soc. 2012, 134, 3748−3757

170.42, 170.06, 169.57, 132.81, 128.92, 128.24, 100.66, 85.70, 76.88, 76.11, 74.01, 73.74, 72.86, 72.00, 70.18, 68.12, 62.41, 62.14, 20.90, 20.87, 20.83. ESI-MS: 662.21 [$(M + NH_4)^+$].

*Phenyl (2,6-Di-O-acetyl-4-O-(^{18}O)acetyl-β-D-galactopyranosyl)-(1→4)-2,3,6-tri-O-acetyl-1-thio-β-D-glucopyranoside (**8**).* A flame-dried flask was charged with **7** (200 mg, 0.31 mmol), dry acetonitrile (10 mL), triethyl orthoacetate (0.3 mL, 1.64 mmol), and *p*-toluenesulfonic acid (10 mg, 0.05 mmol). The resultant solution was stirred at room temperature and TLC analysis showed the reaction to be complete after 30 min, R_f = 0.48 (1:4 v/v acetone/toluene). Following addition of ^{18}O-water (25 μL, 1.24 mmol; 95.1 atom % O-18) to the reaction mixture, stirring was continued for 1 h. After addition of EtOH (5 mL), the volatiles were removed under reduced pressure, and the resulting crude residue was purified by flash chromatography (3:7 v/v acetone/toluene) to afford the desired product as a light yellow syrup (187.9 mg, 0.27 mmol, 88% yield). ^{1}H NMR (600 MHz, $CDCl_3$) δ 7.45−7.36 (m, 2H), 7.28−7.21 (m, 3H), 5.22 (s, 1H), 5.14 (t, *J* = 8.9, 1H), 4.85 (t, *J* = 9.5, 1H), 4.78 (s, 1H), 4.61 (m, 1H), 4..47 (m, 1H), 4.35 (m, 1H), 4.09 (m, 1H), 4.06−3.94 (m, 2H), 3.78−3.54 (m, 4H), 2.11 (s, 3H), 2.10 (s, 3H) 2.07−2.00 (6H, 2 × CH_3), 1.99 (s, 3H), 1.95 (s, 3H); ^{13}C NMR (151 MHz, $CDCl_3$) δ 171.13, 170.71, 170.49, 170.44, 169.86, 169.61, 132.87, 131.97, 128.93, 128.29, 100.77, 85.65, 76.77, 76.20, 73.74, 73.02, 71.61, 70.97, 70.19, 69.19, 62.35, 61.44, 30.98, 20.87, 20.79, 20.70.

*Phenyl (2,6-Di-O-acetyl-4-O-(^{18}O)acetyl-β-D-gulopyranosyl)-(1→4)-2,3,6-tri-O-acetyl-1-thio-β-D-glucopyranoside (**9**).* A solution of **8** (151.6 mg, 0.22 mmol) in dichloromethane (10 mL) was cooled to −78 °C. Upon the addition of pyridine (68.8 μL, 0.85 mmol) and trifluoromethanesulfonic anhydride (74 μL, 0.35 mmol), the mixture was allowed to warm to room temperature. After 30 min, the mixture was successively washed with 1 N HCl (20 mL), sat. $NaHCO_3$ (20 mL), and brine (20 mL). The organic layer was dried (Na_2SO_4) and concentrated under reduced pressure. The resultant crude residue was dissolved in anhydrous DMF and treated with $NaNO_2$ (71 mg, 1.03 mmol). This reaction mixture was stirred overnight at 50 °C. Upon removal of the solvent, the crude residue was purified via flash chromatography (3:7 v/v acetone/toluene) to afford the desired product as a white solid (113.4 mg, 0.17 mmol). Mp = 91−92 °C; ^{1}H NMR (600 MHz, $CDCl_3$) δ 7.55−7.48 (m, 2H), 7.38−7.31 (m, 3H), 5.24 (t, *J* = 9.1, 1H), 4.96 (s, 2H), 4.82 (s, 2H), 4.72 (d, *J* = 10.0, 1H), 4.50 (d, *J* = 13.5, 1H), 4.35−4.24 (m, 2H), 4.21 (s, 1H), 4.13 (d, *J* = 6.4, 2H), 3.79 (t, *J* = 9.5, 1H), 3.68 (m, 1H), 2.33 (m, 1H), 2.15 (s, 9H), 2.12 (s, 3H), 2.11 (s 3H), 2.09 (s, 3H); ^{13}C NMR (151 MHz, CDCl3) δ 171.23, 170.48, 170.22, 170.12, 169.76, 169.69, 132.81, 128.95, 128.28, 98.61, 86.37, 85.86, 76.47, 73.85, 70.92, 70.20, 69.69, 69.41, 67.45, 62.46, 61.42, 20.89, 20.84, 20.73.

*Phenyl (2,3,6-Tri-O-acetyl-β-D-(3-^{18}O)galactopyranosyl)-(1→4)-2,3,6-tri-O-acetyl-1-thio-β-D-glucopyranoside (**10**)).* A solution of **9** (95 mg, 0.14 mmol) in dichloromethane (15 mL) was treated with pyridine (150 μL, 1.85 mmol) and cooled to 0 °C. After addition of trifluoromethanesulfonic anhydride (144 μL, 0.675 mmol), the resultant mixture was warmed to room temperature, and after 4 h, the mixture was washed successively with 1 N HCl (20 mL), sat. $NaHCO_3$ (20 mL), and brine (20 mL). After the organic layer was dried (Na_2SO_4) and concentrated under reduced pressure, the crude residue was dissolved in THF (10 mL) and treated with H_2O (100 μL, 5.5 mmol) and 2,6-lutidine (150 μL, 1.3 mmol). The resultant mixture was and stirred at 40 °C for 1 h, at which time the volatiles were removed under reduced pressure. Purification of the resultant crude residue was accomplished using flash chromatography (3:7 v/v acetone/toluene) to afford the desired product as a white solid (87.4 mg, 0.13 mmol). Mp = 90−92 °C; ^{1}H NMR (600 MHz, $CDCl_3$) δ 7.54−7.48 (m, 2H), 7.37−7.31 (m, 3H), 5.32 (s, 1H), 5.24 (t, *J* = 8.5, 1H), 4.95 (t, *J* = 9.7, 1H), 4.87 (m, 1H), 4.71 (d, *J* = 10.1, 1H), 4.57 (d, *J* = 11.9, 1H), 4.44 (d, *J* = 7.8, 1H), 4.19 (dd, *J* = 5.8, 11.9, 1H), 4.16−4.05 (m, 2H), 3.85−3.73 (m, 3H), −3.69 (m, 1H), 2.54 (d, *J* = 6.3, 1H), 2.20 (s, 3H), 2.15 (s, 3H), 2.14 (s, 3H), 2.12 (s, 3H), 2.09 (s, 3H), 2.06 (s, 3H); ^{13}C NMR (151 MHz, $CDCl_3$) δ 171.44, 170.51, 170.32, 170.22, 169.85, 169.63, 132.90, 131.99, 128.94, 128.28, 100.80, 85.63, 76.22, 73.74, 73.13, 73.08, 71.75, 70.97, 70.19, 69.14, 62.31, 61.39, 20.89, 20.79, 20.69.

*Phenyl ((3-^{18}O)-β-D-Galactopyranosyl)-(1→4)-1-thio-β-D-glucopyranoside (**4b**).* A solution of freshly prepared NaOMe (0.17 M, 20 mL) was added to **10** (80.0 mg, 0.12 mmol) and stirred at room temperature for 5 h. Amberlite IR-120+ resin (H^+ form) was added to neutralize the reaction, and the suspension was stirred for another 15 min before being filtered. The filtrate was concentrated under reduced pressure to afford the desired product as an off-white solid (46.1 mg, 0.11 mmol, 93% yield). The ^{1}H and ^{13}C NMR spectra were identical to those for the unlabeled compound (**4a**) except that the resonance for C3 in the ^{13}C NMR spectrum was shifted upfield by ∼0.021 ppm.

Kinetic Isotope Effect Measurements. The NMR spectroscopic measurements of ^{13}C- and ^{18}O-KIEs, at 25 °C, followed the published protocols[16] except that: (i) deuterium oxide (5 μL, < 1.0% of the final reaction volume) was added directly into the NMR tube containing the labeled substrates (∼1.5−2.0 mg) and buffer (645 μL, 50 mM NaOAc pH 5.5) for signal locking; (ii) automated gradient shimming of the magnetic field using the ^{2}H lock signal was initially performed and this operation was followed by manual shimming, which involved adjusting the various shim currents in order to ensure optimal (symmetric) line shapes in the ^{1}H NMR spectrum (spectra were automatically Fourier transformed in real-time every 3 s during this procedure); and (iii) the amount of VcNA was adjusted such that 80% of the catalyzed reaction was complete within approximately 8 h. To measure β-secondary deuterium KIEs, a simultaneous inverse-gated ^{1}H and ^{2}H decoupling sequence was used during ^{13}C NMR spectral acquisition. Specifically, pulse lengths were measured on the sample and the powers used to calculate pulse power levels for simultaneous 1H and 2H Globally optimized Alternating phase Rectangular Pulse (GARP)[24,25] composite pulse decoupling (CPD). GARP-4 was used to reduce amount of power required for efficient decoupling and to minimize sample heating.[24,25] The spectral width was 240 ppm (36 058 Hz), 102 400 complex points acquired (acquisition time 1.42 s), and a recycle delay 2 s between transients. The dead time after the ^{13}C pulse was set to 20 μs to minimize pulse breakthrough. The ^{13}C transmitter was set to 50 ppm; 12 μs π/2 pulse at 29.6 W was used. The ^{1}H transmitter was set to 4 ppm, GARP-4 CPD used 80 μs pulses at 0.21 W, and the ^{2}H transmitter was set on resonance of the ^{2}H signal (1.76 ppm). GARP-4 CPD used 300 μs pulses at 3.40 W and ^{2}H locking was gated on during the recycle delays but off during FID acquisition. Under these conditions, ^{13}C{^{1}H, ^{2}H} resonances had line widths at half-height of 0.01 ppm or less. Of note, an inverse gated decoupling pulse sequence was used in all KIE experiments to minimize NOE enhancements. In addition, we checked that transient NOE build-up from previous scans did not contribute to the signal intensities by increasing the relaxation delay to >15 × T_1, and showed that under these conditions the measured signal intensities were found to be identical to those measured using our published experimental protocols in which the shorter relaxation delays were utilized.[16]

For all β-secondary ^{2}H-KIEs experiments on the 2,3-diastereomer **2**, a filtered solution of *E. coli* Neu5Ac aldolase was added into the NMR tube in order to reduce the signal intensity of β-Neu5Ac by equilibrating the Neu5Ac generated during the hydrolysis reaction with *N*-acetylmannosamine (ManNAc) and pyruvate.[26] Experimental spectra were fit using the 'deconvolution' function from the Bruker Topspin 2.1 program (fits are provided in Supporting Information). Peaks were fit to a Lorentzian shape, detection sensitivity = 0.5, and peak overlapping factor = 0.5 ppm.

Computational Modeling. Calculations for the VcNA-catalyzed hydrolyses of α-sialosides were determined with Gaussian 09[27] using the B3LYP method with a 6-31G* basis set. The 4-hydroxyl and the 5-*N*-acetamido functional groups as well as the 6-glycerol side chain were removed from the Neu5Ac core in order to generate a truncated substrate. In addition, a methoxy leaving group was used in place of the natural 3- and 6- hydroxyl groups of the terminal galactose residue found in many natural substrates.[28] From several starting geometries, calculations were performed to locate the ground state structure by minimizing its energy in vacuo. Subsequent frequency calculations

Scheme 1. Chemoenzymatic Synthesis of the Isotopologues of 2 and 3 That Were Used for the Measurement of *V*/*K* KIEs on the *V. cholerae* Sialidase-Catalyzed Hydrolyses of Neu5Acα2,3LacβSPh and Neu5Acα2,6LacβSPh

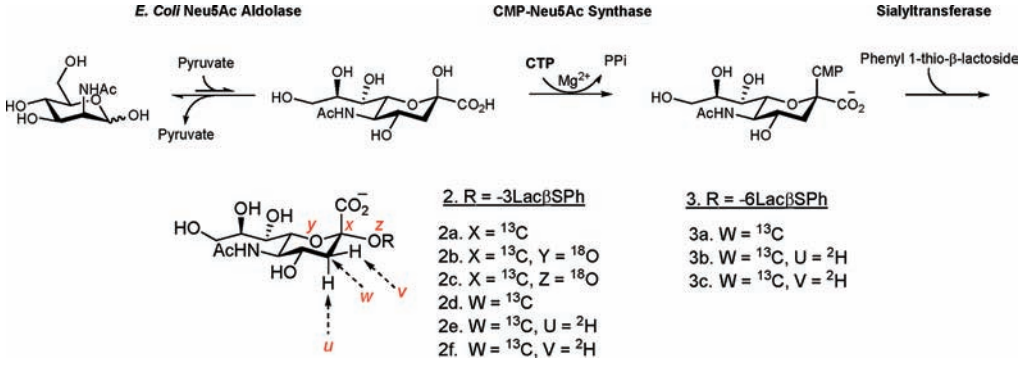

Scheme 2. Synthesis of 3′-^{18}O-1-Thiolactoside[a]

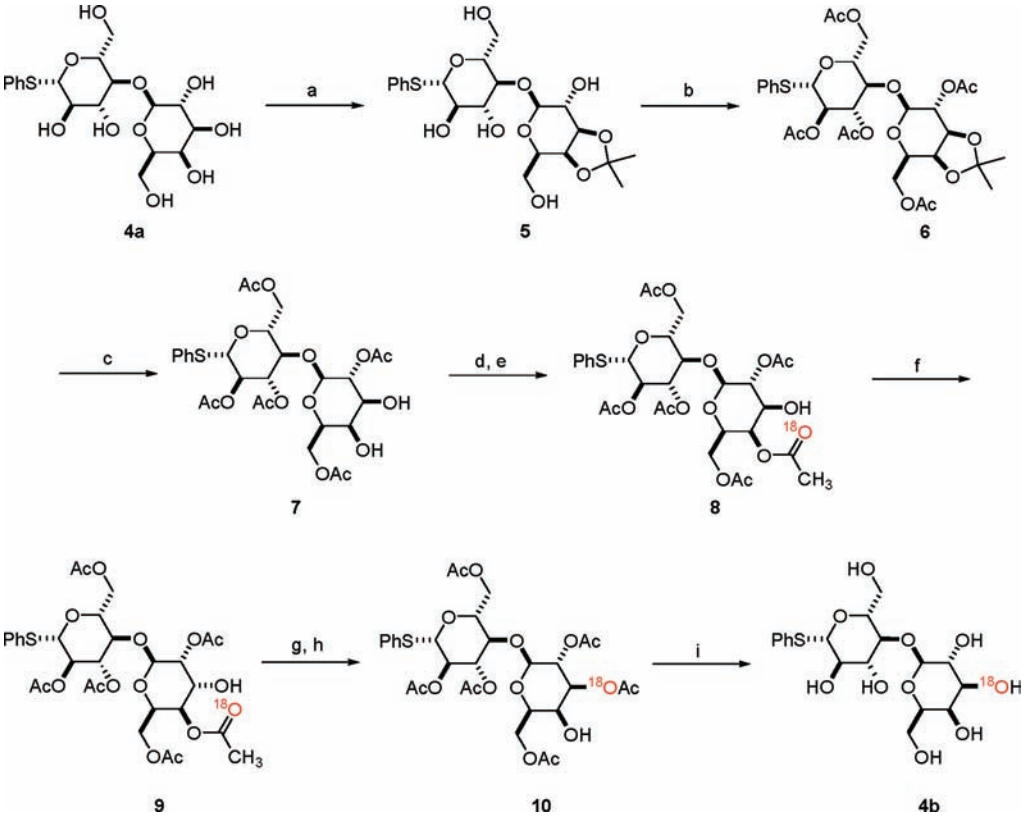

[a]Reagents and conditions: (a) 2,2-dimethoxypropane, H_2SO_4, 55%; (b) pyridine, Ac_2O, 93%; (c) H_2O/AcOH (1:3 v/v), 70 °C, 85%; (d) triethyl orthoacetate, pTSA; (e) $H_2{}^{18}O$ (88% d and e); (f) pyridine, Tf_2O, then $NaNO_2$, 75%; (g) pyridine, Tf_2O; (h) H_2O, 2,6-lutidine (92% g and h); (i) NaOMe/MeOH, 91%.

were shown to have no imaginary frequencies and the geometry of this minima was used in all subsequent KIE calculations.

Likewise, all TS calculations were carried out in vacuo where the three catalytic residues (Asp250, Glu619 and Tyr740) and the presumed transition state analogue inhibitor Neu2en5Ac (5-acetamido-2,6-anhydro-3,5-dideoxy-D-*glycero*-D-*galacto*-non-2-enonic acid; DANA) were imported from the VcNA crystal structure (PDB: 1W0O)[10] into Gaussview 3.0. The structure of the inhibitor (DANA) was truncated in an identical fashion to that used for the substrate before methanol was added across the endocyclic alkene to give a bound substrate analogue. Furthermore, the active site residues Asp250, Glu619, and Tyr740 were truncated to acetic acid, acetate, and *p*-cresol, respectively. In all subsequent calculations, the orientation of the C-1 carboxylate of the truncated sialoside analogue relative to the pyranosyl ring was constrained by fixing one of the O6−C2−C1−O dihedral angles in order to mimic the interaction of this crucial anionic group with the conserved arginine triad. Initially, five structures with a single imaginary frequency, which are consistent with a nucleophilic displacement reaction, were located by first fixing the leaving group (Me)O−C2 bond distance at various distances between 1.60 and 2.10 Å while simultaneously setting the separation between the anomeric carbon and the tyrosinyl oxygen atoms (2.40−3.00 Å) followed by full minimization at the B3LYP/6-31G* level of theory. During these procedures, in order to shorten the distance between the nucleophilic tyrosinyl oxygen and the anomeric carbon atoms, all enzymatic atoms associated with the Tyr/Glu pair were moved the same distance. In other words, no relative motion of this enzymatic dyad was allowed relative to the bound substrate. As a result, this protocol ensured that the H−bond between the ArO−H and the R−CO_2^- remained properly aligned for catalysis. One of the five TS

dx.doi.org/10.1021/ja208564y | *J. Am. Chem. Soc.* 2012, 134, 3748−3757

Table 1. Kinetic Isotope Effects on V/K for the *V. cholerae* Sialidase-Catalyzed Hydrolyses of 1 and 2 in 50 mM NaOAc Buffer pH = 5.5 and T = 25 °C[a]

site of substitution	Neu5Acα2,3LacβSPh (**2**)	Neu5Acα2,6LacβSPh (**3**)	PNP-αNeu5Ac (**1**)
Anomeric 2-^{13}C	1.022 ± 0.001[b]	1.017 ± 0.001[b]	–
Leaving group 2-^{18}O	1.029 ± 0.002	1.039 ± 0.001[b]	1.046 ± 0.015[c]
Ring 6-^{18}O	0.983 ± 0.001	0.975 ± 0.001[b]	–
Equatorial (3*S*)-^{2}H	1.034 ± 0.002[d]	1.021 ± 0.001[e]	1.030 ± 0.017[c]
Axial (3*R*)-^{2}H	1.043 ± 0.002	1.049 ± 0.001[e]	1.030 ± 0.017[c]

[a]Reported values represent weighted averages (n = 3). [b]KIE values taken from ref 16. [c]KIE values taken from ref 14. [d]Reported values represent weighted averages (n = 4). [e]Values for $^{D}V/K_R$ and $^{D}V/K_S$ were determined simultaneously.

structures was chosen for further optimization as it was associated with a leaving group ^{18}O KIE close to the experimental values. These calculations were performed to match the effects at the various heavy-atom positions in the following order: (i) anomeric ^{13}C; (ii) leaving group ^{18}O; and (iii) ring oxygen ^{18}O, with the experimental KIEs being used as constraints. The KIEs associated with each putative TS structure were calculated using the ISOEFF98 program,[28,29] with a scale factor of 0.9614.[30] In addition, four intermediate structures, EIE1−EIE4, were located by further increasing the (Me)O−C2 bond distance of TS3 by 0.25 Å increments until a final distance of 3.00 Å was reached. The corresponding equilibrium isotope effects (EIEs) were then calculated using ISOEFF98 program.

RESULTS AND DISCUSSION

Synthesis of Substrate Isotopologues. The synthetic route used to make the six Neu5Acα2,3LacβSPh and four Neu5Acα2,6LacβSPh isotopologues (Scheme 1) required for the measurement of the six KIE values necessary to complement the reported ^{13}C- and ^{18}O-KIE values[16] for the VcNA-catalyzed hydrolyses of the two natural substrate analogues **2** and **3** is identical to that previously reported.[16] That is, the necessary isotopologues were synthesized chemoenzymatically starting from pyruvate, ManNAc, and LacβSPh using three enzymes, sialic acid aldolase, CMP-sialic acid synthase, and a sialyltransferase (Scheme 1).[16] The labeled starting materials for the isotopically substituted substrates were (i) (2-^{13}C)pyruvate for **2a**; (ii) (2-^{13}C)pyruvate and *N*-acetyl-(3-^{18}O)mannosamine[20] for **2b**; (iii) (2-^{13}C)pyruvate and phenyl (3′-^{18}O)-1-thiolactoside, the synthesis of which is shown in Scheme 2, for **2c**; (iv) (3-^{13}C)pyruvate for **2d** and **3a**; and (v) (3-^{13}C)pyruvate followed by base-catalyzed deuterium incorporation into the (3-^{13}C)sialic acid[22] for **2e**, **2f**, **3b**, and **3c**. In our hands, the base-catalyzed deuterium exchange onto C3 of (3-^{13}C)Neu5Ac resulted in a mixture of Neu5Ac isotopologues (3-H_2, *R*-3-^{2}H, *S*-3-^{2}H, and 3-$^{2}H_2$) with the precise ratios dependent on the pH and time that the exchange reaction was allowed to proceed. Of note, during the preparation of deuterated CMP (3-^{13}C)Neu5Ac under mildly alkaline conditions (pH ∼ 8.5; 37 °C; 90 min), no deuterium washout was observed.

The critical isotopic labeling step in the synthesis of phenyl (3′-^{18}O)-1-thiolactoside (**4b**) was accomplished by the use of a neighboring group assisted solvolysis reaction in which the labeled 4′-*O*-acetyl carbonyl oxygen atom nucleophilically displaced the triflate ester formed from the D-*gulo* configured alcohol **9**. After standard Zemplén deacetylation, the overall yield for this nine-step reaction sequence is 24% (Scheme 2).

Experimental KIEs. It is important to remember that the measured KIEs are on a ^{13}C-containing isotopologue (the NMR active probe nucleus). As a result, the experimental values will be slightly larger than those that would have been measured with substrates that possess the natural abundance isotope ratio at the probe position; however, this perturbation is small (see Supporting Information for a rudimentary analysis of the vibrational frequency differences expected based on a simple diatomic, harmonic oscillator model). The measurement of all V/K KIEs used the recently published NMR spectroscopic methodology (see Experimental Mehods section for full details).[16] For example, the measured ring oxygen $^{18}V/K$ values for the *V. cholerae* sialidase-catalyzed hydrolysis of the 2,3-sialoside, which involved monitoring the competitive reaction between **2a** and **2b**, were 0.9832 (16), 0.9840 (42), and 0.9832 (30) where the standard error, which corresponds to the last two significant figures, is given in parentheses (Figures S1a and S2, Table S1; Supporting Information), while the $^{18}V/K$ values for the leaving group oxygen involving the competition between **2a** and **2c** were 1.0272 (27), 1.0312 (27), and 1.0281 (29) (Figures S1b and S3, Table S2; Supporting Information).

As noted above, we were unable to incorporate deuterium sialic acid stereospecifically into sialic acid; however, the KIEs for both *R*-3-^{2}H and *S*-3-^{2}H diastereomers could be measured on isotopologue mixtures containing **2d**, **2e**, and **2f** (or **3a**, **3b**, and **3c**). Shown in Figure S4 (Supporting Information) are the appropriate ^{13}C chemical shifts of isotopologues **2d**, **2e**, **2f** and the corresponding isotopologues of the hydrolysis product β-sialic acid (of note, the chemical shifts for the anomeric α-sialic acid isotopologues do not interfere with the analysis as they resonate downfield at ∼40.3−40.7 ppm). Representative stacked plots of the changes in isotopologue ratio that occur during the course of VcNA-catalyzed hydrolyses of Neu5Acα2,3LacβSPh are shown in Figure S5 while Figures S6 and S7 display typical mathematical fits of the experimental spectra and Tables S3 and S4 list the full experimental data (Supporting Information). The individually measured $^{D}V/K_S$ effects are 1.0323 (52), 1.0333 (36), 1.0365 (36), and 1.0312 (50), while the corresponding $^{D}V/K_R$ values are 1.0459 (43), 1.0419 (36), and 1.0422 (29). The β-secondary ^{2}H KIEs for Neu5Acα2,6LacβSPh **3** were determined simultaneously as the signals for the product β-Neu5Ac isotopologues are well separated from those of the starting material. Listed in Figure S8 (Supporting Information) are the appropriate ^{13}C chemical shifts of isotopologues **3a**, **3b**, and **3c**, while illustrative stacked plots for the simultaneous measurement of both $^{D}V/K$ values on the hydrolysis of Neu5Acα2,6LacβSPh are shown in Figure S9, Figure S10 displays typical mathematical fits of the experimental spectra, and Table S5 list the full experimental data (Supporting Information). The individually measured $^{D}V/K_S$ effects are 1.0218 (21), 1.0212 (13), and 1.0219 (15), and the $^{D}V/K_R$ KIEs are 1.0492 (18), 1.0483 (18), and 1.0482 (17). Listed in Table 1 are the means and standard deviations[31] for all KIEs determined on the VcNA-catalyzed hydrolyses of Neu5Acα2,3LacβSPh and Neu5Acα2,6LacβSPh.

dx.doi.org/10.1021/ja208564y | *J. Am. Chem. Soc.* 2012, 134, 3748−3757

Intrinsic KIEs. To draw conclusions from competitive KIEs, it is important either to measure or to be able to calculate the intrinsic KIE values, for which contributions from nonchemical and isotopically insensitive steps are negligible.[12] In the present case, it has been shown for VcNA-catalyzed hydrolyses that glycosidic bond cleavage is the kinetically significant step, based on large negative β_{lg} values, for both V and V/K.[14] Of note, the high K_m value reported for sialyl lactose by Ada et al. (1.2 mM)[32] implies weak substrate binding and no commitment to catalysis for the Michaelis complex, a conclusion which requires that a subsequent step is kinetically significant. Accordingly, the measured KIEs listed in Table 1 are concluded to be equal to the intrinsic effects.

Mechanism of Sialidase-Catalyzed Hydrolyses. The recently published mechanism for sialidase-catalyzed hydrolyses (Scheme 3), which is a refinement of previously advocated

Scheme 3. Mechanistic Scheme for Sialidase-Catalyzed Hydrolysis Reactions

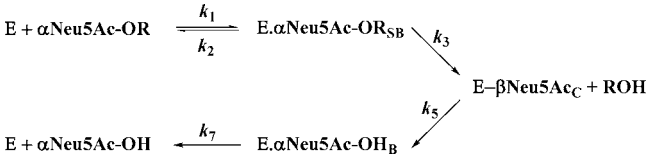

schemes,[14,33−36] is based on a comprehensive series of KIE measurements on the kinetic parameter V_{max} for the *Micromonospora viridifaciens* enzyme.[37] In detail, the bound sugar residue in the accumulating Michaelis complex is in a skew boat conformation (likely the $^6S_2$) with subsequent glycosidic bond cleavage occurring to give a $^1C_4$ chair intermediate that is covalently bound to the active site tyrosine residue.[38] Subsequently, the kinetic significant deglycosylation reaction (V_{max}) occurs with little or no assistance from the nucleophile, which in this case is a solvent water molecule, to give the enzyme/product complex from which the α-sialic acid product dissociates rapidly from the enzyme, before it undergoes mutarotation in solution.[39]

The *V. cholerae* sialidase effectively catalyzes the hydrolysis of a range of naturally occurring glycoconjugates in which the terminal residue is a sialic acid.[40,41] Indeed, VcNA can process both α-(2→3)- and α-(2→6)-glycosidic linkages, albeit with a slight preference for the α-(2→3)-linkage when the penultimate carbohydrate is a galactose residue.[40,41]

(2-^{18}O) and (6-^{18}O) KIEs. For nonenzymatic reactions in water where cleavage of one of the two C−O acetal bonds is rate-limiting, the two ^{18}O-KIEs are typically complementary, that is, the leaving group ^{18}O-KIE is normal ($k_{16}/k_{18} > 1$) while the ^{18}O-KIE associated with formation of the oxacarbenium ion intermediate is inverse ($k_{16}/k_{18} < 1$).[42−44] Similar KIEs are expected to be measured for glycosyl hydrolases in which glycosylation is a kinetically significant step.

With regard to VcNA, the leaving group $^{18}V/K$ values are 1.029 ± 0.002 and 1.039 ± 0.001[16] for **2** and **3**, respectively (cf. 1.046 ± 0.015 for PNP-αNeu5Ac)[14] with the smaller effects being consistent with a greater degree of proton transfer to the leaving group at the glycosylation transition state.[45] Similar results have been reported for the β-glucosidase catalyzed hydrolysis of *p*-nitrophenyl β-D-glucoside, $^{18}V/K$ = 1.0377 ± 0.006.[46] As expected, ring $^{18}V/K$ effects for **2** and **3** are inverse being 0.983 ± 0.001 and 0.975 ± 0.001,[16] respectively. These inverse $^{18}V/K$ values are consistent with an increased anomeric carbon to ring oxygen bond order at the respective TSs with resultant charge delocalization occurring onto the pyranosyl ring oxygen at the glycosylation TS.

(2-^{13}C) KIEs. Although S_N2 reactions, in general, do not occur at tertiary carbon atoms because of steric hindrance to nucleophilic attack, recently, Toney and co-workers concluded that 1,4,7-trimethyloxatriquinane, a 3-fold tertiary alkyl oxonium salt, undergoes a facile S_N2 displacement with azide ion.[47] As a result, it cannot be assumed a priori that sialidases operate via a stepwise mechanism and the anomeric ^{13}C-KIE can be used as a valuable mechanistic probe.[48,49] Typically, concerted S_N2-like reactions feature ^{13}C-KIEs in the range of 1.03−1.08,[50] whereas stepwise S_N1-like reactions ordinarily exhibit smaller ^{13}C-KIE between 1.00 and 1.01.[42,51] With regard to enzyme-catalyzed sialyl transfer, Yang et al. reported an anomeric ^{13}C KIE of 1.032 ± 0.008 for the reaction of sialyl-galactose (Neu5Acα2,3Gal) with the *trans*-sialidase from *Trypanosoma cruzi*,[52] a result that was interpreted in terms of a "*mechanism involving nucleophilic participation in the rate-determining transition state*". In contrast, the previously reported anomeric $^{13}V/K$ values for **2** and **3**, $^{13}V/K$ = 1.022 ± 0.001 and $^{13}V/K$ = 1.017 ± 0.001, respectively,[16] when corrected to $^{14}V/K$ values (1.032−1.042),[53] are consistent with stepwise "exploded" transition states in which the nucleophile attacks an oxacarbenium ion intermediate.[54,55] It thus appears that enzymatic TSs for glycosylation in sialyl transferring enzyme are finely poised with respect to whether the nucleophilic tyrosine has started to attack just prior to (A_ND_N) or immediately following ($D_N^{\ddagger}$*A_N) formation of an oxacarbenium ion.

(3-^2H_R) and (3-^2H_S) β-Secondary KIEs. The measured axial KIEs ($^DV/K_R$) for both **2** and **3** were larger in magnitude than those for equatorial isotopic substitution ($^DV/K_S$), that is 1.043 ± 0.002 versus 1.034 ± 0.002 and 1.049 ± 0.001 versus 1.021 ± 0.001, respectively. The β-secondary ^{2}H-KIEs have traditionally been interpreted as resulting from an angular dependent[56,57] hyperconjugation of an adjacent C−H/D bond into the nascent anomeric p-orbital and these effects have been used to provide insight into sialosyl ring geometry at the enzymatic[14,33,37,52,58] and nonenzymatic[22] TSs. The larger ($^DV/K_R$) effects are consistent with a TS structure for glycosylation in which the anomeric center has been flattened and is likely close to the predicted $^4H_5$ half-chair conformation.[59]

Computational Modeling of Transition States. All calculations were performed at the B3LYP/6-31G* level with the ground state and transition states being in vacuo. The geometry of the truncated substrate was optimized without constraints with a $^2C_5$ chair conformation (Figures S11 and Table S6, Supporting Information). For TS calculations, because of the significant interaction upon substrate binding to the sialidase active site involving formation of a strong salt-bridge[60] between the C-1 carboxylate of the substrate and the three strictly conserved enzymatic arginine residues, which are Arg224, Arg635, and Arg712 in VcNA,[10] it was decided to restrict the motion of the carboxylate group during modeling. During the modeling exercise, using the experimental heavy-atom KIEs as constraints, four TS structures were located for the VcNA-catalyzed hydrolysis of the 2,3-isomer, whereas only a single TS could be located for the corresponding reaction on the 2,6-isomer. Indeed, due to the numerous constraints that were required to: (i) freeze the substrate carboxylate group and stop it forming an α-lactone during minimization; and (ii) stop the cresol group, which mimics the enzymatic tyrosine

dx.doi.org/10.1021/ja208564y | J. Am. Chem. Soc. 2012, 134, 3748−3757

nucleophile, from forming π-cation complexes with the developing charge on the oxacarbenium ion fragment, numerous calculations failed to converge.

Tables 2 and 3 list the calculated KIEs and the corresponding experimental values, with the NMR probe ^{13}C nucleus

Table 2. Calculated KIEs Including the ^{13}C Probe Atom, at the B3LYP/6-31G* Level of Theory, for the *V. cholerae* Sialidase-Catalyzed Hydrolyses of Neu5Acα2,3LacβSPh in 50 mM NaOAc Buffer pH = 5.5 and T = 25 °C

isotopologue	TS1	TS2	TS3	TS4	experimental
Ring 6-^{18}O	0.9816	0.9795	0.9813	0.9820	0.983 ± 0.001
Anomeric 2-^{13}C	1.0265	1.0247	1.0200	1.0234	1.022 ± 0.001
Leaving group 2-^{18}O	1.0467	1.0283	1.0219	1.0281	1.029 ± 0.002
Equatorial (3*S*)-^{2}H	1.0223	0.9968	0.9857	0.9974	1.034 ± 0.002
Axial (3*R*)-^{2}H	0.9404	0.9537	0.9081	0.9122	1.043 ± 0.002

Table 3. Calculated KIEs Including the ^{13}C Probe Atom, at the B3LYP/6-31G* Level of Theory, for the *V. cholerae* Sialidase-Catalyzed Hydrolyses of Neu5Acα2,6LacβSPh in 50 mM NaOAc Buffer pH = 5.5 and T = 25 °C

isotopologue	TS5	experimental
Ring 6-^{18}O	0.9779	0.975 ± 0.001
Anomeric 2-^{13}C	1.0189	1.017 ± 0. 001
Leaving group 2-^{18}O	1.0364	1.039 ± 0.001
Equatorial (3*S*)-^{2}H	0.9444	1.021 ± 0.001
Axial (3*R*)-^{2}H	0.8686	1.049 ± 0.001

implicitly included in the computation, for the transition state structures located during the modeling of the truncated and constrained sialic acid analogue for the 2,3- and 2,6-isomers, respectively (Table S7, Supporting Information lists the calculated KIEs when the probe ^{13}C nucleus is replaced by a ^{12}C-atom, while Tables S8−S12 list the Cartesian coordinates of the TS models). Of note, all computed TSs are compatible with a dissociative mechanism, $D_N^{\ddagger}*A_N$,[61] in which the anomeric carbon to nucleophilic oxygen distances are consistent with a negligible C−O bond order (Table 4).[55]

Interestingly, the two modeled 2,3-isomer transition states (models 1 and 2; Figure S12, Supporting Information), where the general acid proton was constrained to its starting position, that is, affixed to the aspartic acid residue, have calculated anomeric carbon KIEs that are remarkably similar despite the differences in the computed distances from the central carbon to both the leaving group and nucleophilic oxygen atoms (Table 4, bond and torsional angles are given in Table S13 in the Supporting Information section). The notable difference in calculated KIEs between these two models is the leaving group ^{18}O value, which clearly is a manifestation of the longer C−O bond (TS1 1.927 versus TS2 1.700 Å). These two TS models were then used as starting points for subsequent minimization calculations after the constraints on the two catalytic protons were removed. Unfortunately, only model #1 could be successfully refined, and this calculation gave TS3 (Figure 1a). Of note, during refinement, the aspartic acid proton underwent transfer to the methoxy leaving group, whereas, essentially, no change has occurred to the position of the tyrosinyl proton. That the proton located between the tyrosine and glutamic acid residues remains steadfastly bonded to the phenolic oxygen atom suggests a mechanistic commonality between the glycosylation and the deglycosylation[37] reactions. That is, both involve dissociative mechanisms in which the two proton transfers occur individually on sequential steps (Scheme 4).

Clearly, transfer of the general-acid proton to the leaving group results in a dramatic decrease in the computed ^{18}O-KIE and a slight attenuation in the anomeric carbon effect (models 1 and 3). A fourth transition state structure (TS4, Figure 1b) was located for the 2,3-isomer, and in essence, this structure is similar to model 3 in which the anomeric carbon to leaving group bond is largely broken with an associated transfer of the general acid proton. In contrast, only a single computed transition state (TS5; Figure S13, Supporting Information) was located in which there was reasonable agreement to the 3 experimental heavy-atom KIEs. Of note, in this transition state for the catalyzed hydrolysis of Neu5Acα2,6βSPh, transfer of the general acid proton to the leaving group has not been initiated. That is, the significant difference in the experimental leaving group $^{18}V/K$ values (1.029, -2,3- vs 1.039, -2,6-, Table 1) is consistent with a greater degree of uncoupling, to glycosidic bond cleavage, of the proton transfer in the TS.

Remarkably, the two closest matches to the experimental heavy-atom KIE data (TS2 and TS4, Table 2) have different spatial arrangements around the anomeric center (Table 4 and Table S13). That two strikingly different TS structures are consistent with the experimental data suggests that in the vicinity of the glycosylation transition state the free energy profile is quite flat. Of note, the ring conformation of TS4, which has the best fit to the experimental data, is best described as a flattened $^{4}H_5$ half-chair (Figure 2a). It can be seen from the dihedral angle about the anomeric carbon−ring oxygen atom (C3−C2−O6-C6, Table S13) that the five TSs are grouped into two conformations both of which are $^{4}H_5$ half-chairs with transition states 3−5 adopting a more flattened conformation than is the case for TS1 and TS2 (Figure 2b).

In addition, we evaluated whether the corresponding β-secondary deuterium EIEs (K_H/K_D) would be normal at extended C−O bond distances (Tables S14−S17, Supporting Information lists the Cartesian coordinates of four such models, Table S18 lists the calculated EIEs, and Table S19 gives

Table 4. Calculated Distances (Å) for All Computed Transition States for the *V. cholerae* Sialidase-Catalyzed Hydrolyses of Neu5Acα2,3LacβSPh (Models 1−4) and Neu5Acα2,6LacβSPh (Model 5)

model no.	O6−C2	O2−C2	C2−Tyr(O)	O2−Asp(H)	Asp(O)−Asp(H)	Tyr(O)−Tyr(H)	Glu(O)−Tyr(H)
1	1.271	1.927	2.700	1.417	1.110	1.017	1.657
2	1.285	1.700	2.500	1.417	1.110	1.017	1.657
3	1.271	1.927	2.700	1.042	1.519	1.018	1.640
4	1.271	1.987	2.700	1.100	1.431	1.019	1.636
5	1.290	1.700	2.498	1.416	1.110	1.016	1.657

dx.doi.org/10.1021/ja208564y | J. Am. Chem. Soc. 2012, 134, 3748−3757

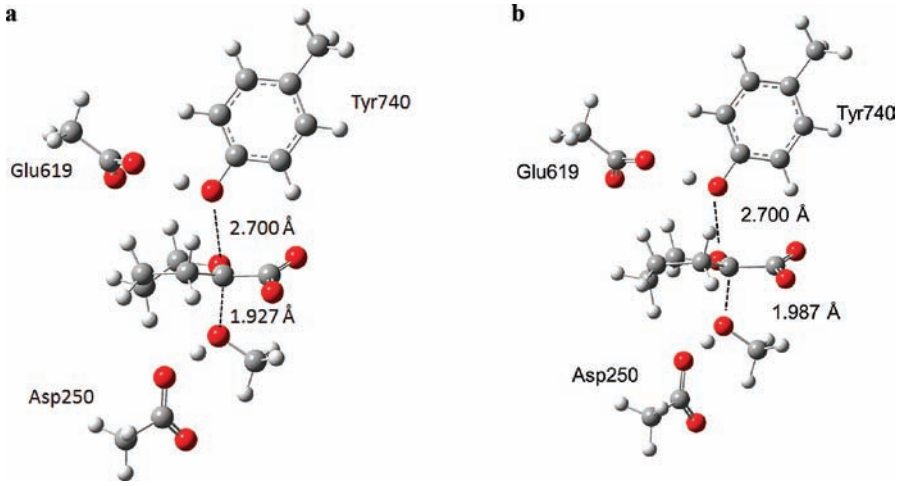

Figure 1. Two transition state structures of VcNA, which were determined in vacuo by hybrid density functional theory implemented in Gaussian 09 using B3LYP functional and the 6-31G(d) basis sets. Panel a displays TS model 3, while panel b shows TS model 4. The distances in the reaction coordinate (C′−O(Tyr) and C′−O(Me) for both transition states are shown.

Scheme 4. Postulated Mechanism for Formation and Breakdown of the Tyrosinyl Bound Intermediate Where the Oxacarbenium Ion May or May Not Have a Lifetime Longer than a Single Vibration[a]

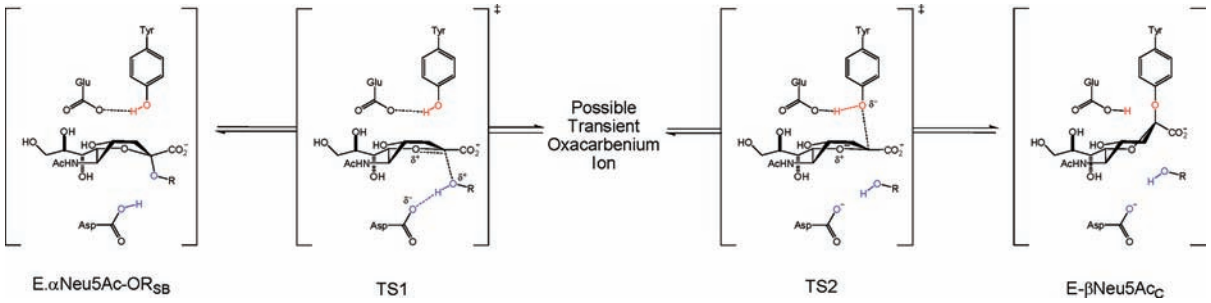

[a]TS1 is based on this work when glycosylation (R = carbohydrate) is kinetically significant, while TS2 is the suggested transition state (R = H, reference 37) for kinetically significant deglycosylation (*M. viridifaciens* sialidase).

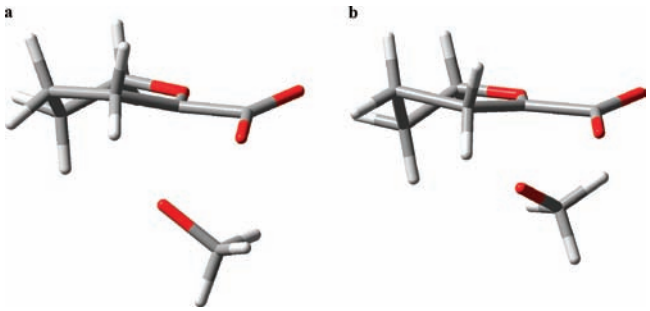

Figure 2. Ring conformations of TS4 (a) and TS2 (b) determined in vacuo by hybrid density functional theory implemented in Gaussian 09 using B3LYP functional and the 6-31G(d) basis sets. The enzymatic residues have been removed for clarity.

selected bond and torsional angles for these structures). Of note, at a distance of 2.25 Å, the equatorial β-secondary EIE became normal, and at 2.75 Å, the axial β-secondary deuterium EIE also became normal. In contrast to TS1−TS5 where the C3−C2−O6−C6 dihedral was slightly negative, the corresponding dihedral for EIE4 was positive (9.79°). To determine whether this geometric parameter was linked to the calculation of normal β-secondary deuterium isotope effects, we performed additional calculations by varying this angle from 9.79−3.79 in 2.0° increments while maintaining the leaving group C−O parameter constrained to the distance located in TS3. Two of these calculations minimized (5.59 and 3.59°), but in both cases, the calculated $^{D}V/K$ KIEs were still inverse (data not shown). We note that qualitatively for a $^{4}H_{5}$ half-chair TS conformation the $^{D}V/K_{R}$ effect should be larger than the corresponding $^{D}V/K_{S}$ value, which is the case (Table 1).[14,33,42]

In summary, the computational modeling of the secondary deuterium KIEs suggests that the TSs for the VcNA-catalyzed hydrolyses may be more dissociative than our computed transition states (TS2−4), which give heavy-atom KIEs that match the experimental values. However, given the degree of truncation needed to keep the system at a reasonable number of atoms, we decided that it was preferable to match the heavy-atom KIEs and that complete matching of computational and experimental values would be problematic until all six critical active site residues (tyrosine, glutamate, aspartate, and the three arginines, which bind the carboxylate group of the substrate) and the enzyme framework that mediates catalysis are incorporated into a QM/MM type calculation.

■ CONCLUSIONS

The transition-state structures for the *V. cholerae* sialidase-catalyzed hydrolysis of two natural substrate analogues were determined by means of quantum chemistry computation using as restraints the experimental KIEs. The mechanism of glycosylation can best be described as dissociative with the

dx.doi.org/10.1021/ja208564y | *J. Am. Chem. Soc.* 2012, 134, 3748−3757

transition states being en route to a $^4H_5$ half-chair oxacarbenium ion.

■ ASSOCIATED CONTENT

Supporting Information

Full author list for refs 4 and 27, representative NMR spectra for the measurement of all KIES, compiled lists of isotopologue chemical shifts used in the KIE measurements, ball and stick diagrams for TS1, TS2, TS5 and the ground state, Cartesian coordinates and the sum of electronic and zero-point energies for all TSs and the ground state, and a derivation of vibrational frequency changes on incorporation of a ^{13}C probe atom. This material is available free of charge via the Internet at http://pubs.acs.org.

■ AUTHOR INFORMATION

Corresponding Author

bennet@sfu.ca

Notes

The authors declare no competing financial interest.

■ ACKNOWLEDGMENTS

The authors thank Prof. Vern Schramm, Dr. Matthew Vetticatt and Dr. Jennifer Hirschi (Albert Einstein College of Medicine) for providing computational training to J.C., and Dr. M. Gilbert and Marie-France Karwaski (Institute for Biological Sciences, National Research Council Canada, Ottawa, Ontario, Canada) for providing the 2,6-sialyltransferase and Dr. Rainer Kummerle (Bruker Switzerland) for assistance with pulse sequence implementation and development. This work was supported by a Natural Sciences and Engineering Research Council of Canada Discovery Grant.

■ REFERENCES

(1) Faruque, S. M.; Nair, G. B. *Vibrio cholerae: Genomics and Molecular Biology*; Caister Academic Press: Norfolk, 2008.
(2) Butler, D. *Nature* **2010**, *468*, 483−484.
(3) Enserink, M. *Science* **2010**, *330*, 738−739.
(4) Mutreja, A.; et al. *Nature* **2011**, *477*, 462−465.
(5) Fishman, P. H. *J. Membr. Biol.* **1982**, *69*, 85−97.
(6) Crennell, S.; Garman, E.; Laver, G.; Vimr, E.; Taylor, G. *Structure* **1994**, *2*, 535−544.
(7) Holmgren, J.; Lonnroth, I.; Mansson, J. E.; Svennerholm, L. *Proc. Natl. Acad. Sci. U.S.A.* **1975**, *72*, 2520−2524.
(8) Galen, J. E.; Ketley, J. M.; Fasano, A.; Richardson, S. H.; Wasserman, S. S.; Kaper, J. B. *Infect. Immun.* **1992**, *60*, 406−415.
(9) Connaris, H.; Crocker, P. R.; Taylor, G. L. *J. Biol. Chem.* **2009**, *284*, 7339−7351.
(10) Moustafa, I.; Connaris, H.; Taylor, M.; Zaitsev, V.; Wilson, J. C.; Kiefel, M. J.; von Itzstein, M.; Taylor, G. *J. Biol. Chem.* **2004**, *279*, 40819−40826.
(11) Schramm, V. L. *Curr. Opin. Struct. Biol.* **2005**, *15*, 604−613.
(12) Berti, P. J.; Tanaka, K. S. E. *Adv. Phys. Org. Chem.* **2002**, *37*, 239−314.
(13) Schramm, V. L. *Annu. Rev. Biochem.* **1998**, *67*, 693−720.
(14) Guo, X.; Sinnott, M. L. *Biochem. J.* **1993**, *294*, 653−656.
(15) Menger, F. M.; Ladika, M. *J. Am. Chem. Soc.* **1987**, *109*, 3145−3146.
(16) Chan, J.; Lewis, A. R.; Gilbert, M.; Karwaski, M. F.; Bennet, A. J. *Nat. Chem. Biol.* **2010**, *6*, 405−407.
(17) Karwaski, M. F.; Wakarchuk, W. W.; Gilbert, M. *Protein Expression Purif.* **2002**, *25*, 237−240.
(18) Kakuta, Y.; Okino, N.; Kajiwara, H.; Ichikawa, M.; Takakura, Y.; Ito, M.; Yamamoto, T. *Glycobiology* **2008**, *18*, 66−73.
(19) Pukin, A. V.; Weijers, C. A. G. M.; van Lagen, B.; Wechselberger, R.; Sun, B.; Gilbert, M.; Karwaski, M. F.; Florack, D. E. A.; Jacobs, B. C.; Tio-Gillen, A. P.; van Belkum, A.; Endtz, H. P.; Visser, G. M.; Zuilhof, H. *Carbohydr. Res.* **2008**, *343*, 636−650.
(20) Indurugalla, D.; Bennet, A. J. *Can. J. Chem.* **2008**, *86*, 1005−1009.
(21) Mahmoudian, M.; Noble, D.; Drake, C. S.; Middleton, R. F.; Montgomery, D. S.; Piercey, J. E.; Ramlakhan, D.; Todd, M.; Dawson, M. J. *Enzyme Microb. Tech.* **1997**, *20*, 393−400.
(22) Ashwell, M.; Guo, X.; Sinnott, M. L. *J. Am. Chem. Soc.* **1992**, *114*, 10158−10166.
(23) Yan, F. Y.; Wakarchuk, W. W.; Gilbert, M.; Richards, J. C.; Whitfield, D. M. *Carbohydr. Res.* **2000**, *328*, 3−16.
(24) Shaka, A. J.; Barker, P. B.; Freeman, R. *J. Magn. Reson.* **1985**, *64*, 547−552.
(25) Shaka, A. J.; Keeler, J. *Prog. Nucl. Magn. Reson. Spectrosc.* **1987**, *19*, 47−129.
(26) Kim, M. J.; Hennen, W. J.; Sweers, H. M.; Wong, C. H. *J. Am. Chem. Soc.* **1988**, *110*, 6481−6486.
(27) Frisch, M. J.; et al. *Gaussian 09*, Revision A.02; Gaussian, Inc.: Wallingford, CT, 2009.
(28) Sander-Wewer, M.; Schauer, R.; Corfield, A. P. *Adv. Exp. Med. Biol.* **1982**, *152*, 215−222.
(29) Anisimov, V.; Paneth, P. *J. Math. Chem.* **1999**, *26*, 75−86.
(30) Scott, A. P.; Radom, L. *J. Phys. Chem.* **1996**, *100*, 16502−16513.
(31) Taylor, J. R. *An Introduction to Error Analysis: The Study of Uncertainties in Physical Measurements*; University Science Books: Mill Valley, CA., 1982.
(32) Ada, G. L.; Lind, P. E.; French, E. L. *J. Gen. Microbiol.* **1961**, *24*, 409−421.
(33) Guo, X.; Laver, W. G.; Vimr, E.; Sinnott, M. L. *J. Am. Chem. Soc.* **1994**, *116*, 5572−5578.
(34) Watson, J. N.; Dookhun, V.; Borgford, T. J.; Bennet, A. J. *Biochemistry* **2003**, *42*, 12682−12690.
(35) Watson, J. N.; Knoll, T. L.; Chen, J. H.; Chou, D. T. H.; Borgford, T. J.; Bennet, A. J. *Biochem. Cell. Biol.* **2005**, *83*, 115−122.
(36) Watts, A. G.; Withers, S. G. *Can. J. Chem.* **2004**, *82*, 1581−1588.
(37) Chan, J.; Lu, A.; Bennet, A. J. *J. Am. Chem. Soc.* **2011**, *133*, 1877−1884.
(38) Watts, A. G.; Oppezzo, P.; Withers, S. G.; Alzari, P. M.; Buschiazzo, A. *J. Biol. Chem.* **2006**, *281*, 4149−4155.
(39) Chan, J.; Sandhu, G.; Bennet, A. J. *Org. Biomol. Chem.* **2011**, *9*, 4818−4822.
(40) Chokhawala, H. A.; Yu, H.; Chen, X. *ChemBioChem* **2007**, *8*, 194−201.
(41) Corfield, A. P.; Higa, H.; Paulson, J. C.; Schauer, R. *Biochim. Biophys. Acta* **1983**, *744*, 121−126.
(42) Bennet, A. J.; Sinnott, M. L. *J. Am. Chem. Soc.* **1986**, *108*, 7287−7294.
(43) Bennet, A. J.; Sinnott, M. L.; Wijesundera, W. S. S. *J. Chem. Soc., Perkin Trans. 2* **1985**, 1233−1236.
(44) Indurugalla, D.; Bennet, A. J. *J. Am. Chem. Soc.* **2001**, *123*, 10889−10898.
(45) Bennet, A. J.; Davis, A. J.; Hosie, L.; Sinnott, M. L. *J. Chem. Soc., Perkin Trans. 2* **1987**, 581−584.
(46) Rosenberg, S.; Kirsch, J. F. *Biochemistry* **1981**, *20*, 3189−3196.
(47) Mascal, M.; Hafezi, N.; Toney, M. D. *J. Am. Chem. Soc.* **2010**, *132*, 10662−10664.
(48) Stivers, J. T.; Werner, R. M. *Biochemistry* **2000**, *39*, 14054−14064.
(49) Luo, M.; Schramm, V. L. *J. Am. Chem. Soc.* **2008**, *130*, 2649−2655.
(50) Zhang, Y.; Bommuswamy, J.; Sinnott, M. L. *J. Am. Chem. Soc.* **1994**, *116*, 7557−7563.
(51) Lee, J. K.; Bain, A. D.; Berti, P. J. *J. Am. Chem. Soc.* **2004**, *126*, 3769−3776.
(52) Yang, J.; Schenkman, S.; Horenstein, B. A. *Biochemistry* **2000**, *39*, 5902−5910.

(53) Melander, L. C. S.; Saunders, W. H. J. *Reaction Rates of Isotopic Molecules*; Wiley: New York, 1980.
(54) Zhang, Y.; Luo, M. K.; Schramm, V. L. *J. Am. Chem. Soc.* **2009**, *131*, 4685−4694.
(55) Schwartz, P. A.; Vetticatt, M. J.; Schramm, V. L. *J. Am. Chem. Soc.* **2010**, *132*, 13425−13433.
(56) Sunko, D. E.; Hirsl-Starcevic, S.; Pollack, S. K.; Hehre, W. J. *J. Am. Chem. Soc.* **1979**, *101*, 6163−6170.
(57) Sunko, D. E.; Szele, I.; Hehre, W. J. *J. Am. Chem. Soc.* **1977**, *99*, 5000−5005.
(58) Chong, A. K. J.; Pegg, M. S.; Taylor, N. R.; von Itzstein, M. *Eur. J. Biochem.* **1992**, *207*, 335−343.
(59) Vocadlo, D. J.; Davies, G. J. *Curr. Opin. Chem. Biol.* **2008**, *12*, 539−555.
(60) Taylor, N. R.; von Itzstein, M. *J. Med. Chem.* **1994**, *37*, 616−624.
(61) Guthrie, R.; Jencks, W. P. *Acc. Chem. Res.* **1989**, *22*, 343−349.